IMAGING INFORMATICS AND ARTIFICIAL INTELLIGENCE

Machine learning based on clinical characteristics and chest CT quantitative measurements for prediction of adverse clinical outcomes in hospitalized patients with COVID-19

Zhichao Feng [1,2] · Hui Shen [3] · Kai Gao [3] · Jianpo Su [3] · Shanhu Yao [1,2] · Qin Liu [1] · Zhimin Yan [1] · Junhong Duan [1] · Dali Yi [1] · Huafei Zhao [1] · Huiling Li [1] · Qizhi Yu [4] · Wenming Zhou [5] · Xiaowen Mao [6] · Xin Ouyang [7] · Ji Mei [8] · Qiuhua Zeng [9] · Lindy Williams [10] · Xiaoqian Ma [1,2] · Pengfei Rong [1,2] · Dewen Hu [3] · Wei Wang [1,2]

Abstract

Objectives To develop and validate a machine learning model for the prediction of adverse outcomes in hospitalized patients with COVID-19.

Methods We included 424 patients with non-severe COVID-19 on admission from January 17, 2020, to February 17, 2020, in the primary cohort of this retrospective multicenter study. The extent of lung involvement was quantified on chest CT images by a deep learning–based framework. The composite endpoint was the occurrence of severe or critical COVID-19 or death during hospitalization. The optimal machine learning classifier and feature subset were selected for model construction. The performance was further tested in an external validation cohort consisting of 98 patients.

Results There was no significant difference in the prevalence of adverse outcomes (8.7% vs. 8.2%, $p = 0.858$) between the primary and validation cohorts. The machine learning method extreme gradient boosting (XGBoost) and optimal feature subset including lactic dehydrogenase (LDH), presence of comorbidity, CT lesion ratio (lesion%), and hypersensitive cardiac troponin I (hs-cTnI) were selected for model construction. The XGBoost classifier based on the optimal feature subset performed well for the prediction of developing adverse outcomes in the primary and validation cohorts, with AUCs of 0.959 (95% confidence interval [CI]: 0.936–0.976) and 0.953 (95% CI: 0.891–0.986), respectively. Furthermore, the XGBoost classifier also showed clinical usefulness.

Conclusions We presented a machine learning model that could be effectively used as a predictor of adverse outcomes in hospitalized patients with COVID-19, opening up the possibility for patient stratification and treatment allocation.

Zhichao Feng and Hui Shen contributed equally to this work.

✉ Dewen Hu
dwhu@nudt.edu.cn

✉ Wei Wang
cjr.wangwei@vip.163.com

1 Department of Radiology, Third Xiangya Hospital, Central South University, No. 138 Tongzipo Road, Changsha 410013, Hunan, China

2 Molecular Imaging Research Center, Central South University, Changsha, Hunan, China

3 College of Intelligence Science and Technology, National University of Defense Technology, No. 109 Deya Road, Changsha 410073, Hunan, China

4 Department of Radiology, First Hospital of Changsha, Changsha, Hunan, China

5 Department of Medical Imaging, First Hospital of Yueyang, Yueyang, Hunan, China

6 Department of Medical Imaging, Central Hospital of Shaoyang, Shaoyang, Hunan, China

7 Department of Radiology, Central Hospital of Xiangtan, Xiangtan, Hunan, China

8 Department of Radiology, Second Hospital of Changde, Changde, Hunan, China

9 Department of Radiology, Central Hospital of Loudi, Loudi, Hunan, China

10 Centre for Transplant and Renal Research, University of Sydney, Westmead, Australia

🍎 Springer

Key Points

• *Developing an individually prognostic model for COVID-19 has the potential to allow efficient allocation of medical resources.*
• *We proposed a deep learning–based framework for accurate lung involvement quantification on chest CT images.*
• *Machine learning based on clinical and CT variables can facilitate the prediction of adverse outcomes of COVID-19.*

Abbreviations

COVID-19	Coronavirus disease 2019
CT	Computed tomography
DL	Deep learning
GGO	Ground-glass opacification
hs-cTnI	Hypersensitive cardiac troponin I
LDH	Lactic dehydrogenase
lr	Logistic regression
RF	Random forest
SVM-Linear	Support vector machine with a linear kernel
SVM-RBF	Support vector machine with a radial basis function
XGBoost	Extreme gradient boosting

Introduction

The coronavirus disease 2019 (COVID-19), with its outbreak and rapid escalation, which range from the common cold to severe or even fatal respiratory infections caused by severe acute respiratory syndrome coronavirus 2 (SARS-CoV-2), has become a worldwide pandemic involving 188 countries or regions and more than 50 million individuals. About 10–20% of COVID-19 patients deteriorate to severe or critical illnesses within 7–14 days after symptom onset, characterized by acute respiratory distress syndrome (ARDS) and/or even multiorgan dysfunction syndrome (MODS), who require more intensive medical resource utilization, tend to develop nosocomial complications, and have worse prognosis with a case fatality rate about 20 times higher than that of non-severe patients [1–3]. There is no specific anti-coronavirus treatment for severe patients at present, and whether remdesivir is associated with significant clinical benefits for severe COVID-19 still requires further confirmation [4, 5]. Nevertheless, early antiviral therapy has been reported to be helpful in alleviating symptoms and shortening the duration of viral shedding in patients with mild to moderate COVID-19 [6, 7]. Thus, the key step in reducing the mortality from COVID-19 should be the prevention of progression from non-severe to severe disease stage and the subsequent development of critical illness. Early identification of patients at risk of adverse outcomes has the potential to enable more individualized treatment plans, but it is difficult for physicians solely based on their clinical experience [8, 9].

There have been several prognostic models in predicting adverse outcomes for COVID-19; however, most were established based on clinical biochemical parameters and few incorporated chest CT imaging features [10–12]. Chest CT is an exclusive tool to assess lung injury, which is the major hallmark of COVID-19 [13]. To accurately quantify the extent of lung injury using CT images, deep learning (DL)–based artificial intelligence (AI) technique may be an optimal solution, which has the advantages of good reproducibility, less time-consuming, and relieving the health systems overloads. Zhang et al have developed a clinically applicable AI system that can distinguish COVID-19 pneumonia from other common pneumonia and provide clinical prognosis for predicting the progression to critical illness and survival probability [14]. However, the clinical feasibility and benefit of machine learning–based model in the early prediction of the progression from non-severe to severe or critical illnesses in COVID-19 patients remain unclear.

In this study, we retrospectively included patients with non-severe COVID-19 at the time of admission from multiple institutes, quantified the extent of lung injury on chest CT images using DL-based framework, constructed a machine learning model incorporating clinical characteristics and CT-derived quantitative measurement to identify the cases who developed adverse outcomes during hospitalization, determined the prediction performance and clinical use benefit, and validated these findings in an independent external cohort (Fig. 1).

Materials and methods

Study population

The Institutional Review Board of the Third Xiangya Hospital approved our study and waived the informed consent of patients for the retrospective nature of this study. The study was conducted according to the TRIPOD recommendations for prediction model development and validation [15]. Consecutive hospitalized patients with confirmed COVID-19 infection who underwent chest CT scan on admission at the Third Xiangya Hospital, First Hospital of Changsha, First Hospital of Yueyang, Second Hospital of Changde, Central Hospital of Xiangtan, Central Hospital of Shaoyang, and Central Hospital of Loudi between January 17, 2020, and February 17, 2020, were screened ($n = 604$). Patients who had severe or critical illnesses on admission ($n = 45$) and were
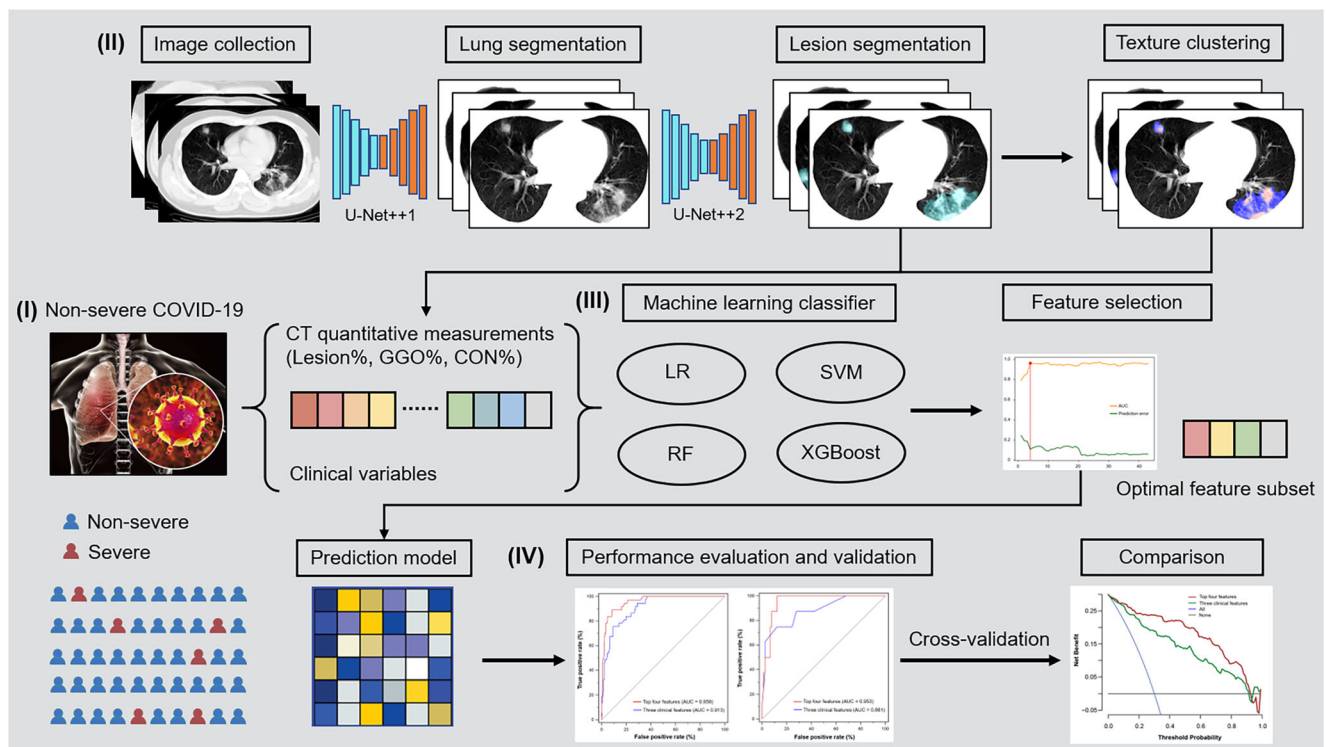
Fig. 1 Study workflow. (I) Non-severe COVID-19 patients who underwent chest CT scan on admission were included. (II) Lung and lesion segmentation were performed using DL-based framework and texture clustering was used to distinguish between GGO and CON. CT quantitative measurements including lesion%, GGO%, and CON% were calculated. (III) The optimal machine learning classifier and feature subset were selected and used for prediction model construction. (IV) The performance of the machine learning model was determined and validated in an external cohort. CON, consolidation; COVID-19, coronavirus disease 2019; CT, computed tomography; DL, deep learning; GGO, ground-glass opacification; LR, logistic regression; RF, random forest; SVM, support vector machine; XGBoost, extreme gradient boosting

younger than 18 years old (*n* = 37) were excluded. A total of 522 patients were ultimately included in this multicentre study and divided into the primary and validation cohorts according to their origin of hospital (Supplementary Figure 1). The criteria for the diagnosis and severity classification of COVID-19 infection are provided in the Supplementary Material.

Data collection

The clinical and laboratory data were obtained with data collection forms from electronic medical records. To accurately quantify the extent of lung involvement on the non-contrast chest CT images, we adopted a U-Net++ DL network developed by our team for the three-dimensional segmentation of lung and lesions (Supplementary Figure 2) [16]. Furthermore, we proposed an unsupervised multi-scale texture feature clustering method to distinguish between ground-glass opacification (GGO) and consolidation (CON) [17]. The CT lesion ratio (lesion%), GGO ratio (GGO%), and CON ratio (CON%) were then calculated, respectively. The details of data collection and CT image analysis are provided in the Supplementary Material.

Machine learning classifier and feature selection

The composite endpoint was the occurrence of severe or critical illnesses or death. The candidate feature set included 43 clinical characteristics or CT quantitative measurements, and Pearson's correlations between features were calculated. To establish an optimal prognostic model to predict the occurrence of the composite endpoint, five supervised machine learning classifiers, namely logistic regression (LR), support vector machine with a linear kernel (SVM-Linear), SVM with a radial basis function (SVM-RBF), random forest (RF), and extreme gradient boosting (XGBoost), were employed to determine a classifier with the best performance [18]. Fivefold cross-validation was performed in the primary cohort and grid search was used for parameter tuning or hyperparameter optimization. Class weight was set at 10 to reduce the influence of inter-group unbalanced distribution. Furthermore, the average feature importance rank that indicated how valuable each feature was in the optimal classifier overall folds of cross-validation in the primary cohort was provided. With the ranked features, different feature subsets could be obtained by selecting top-*n* features from the ordered sequence (*n* = 1~43). The optimal feature subset with the highest prediction

performance and minimum feature numbers was finally selected.

Model establishment and performance evaluation

The optimal machine learning classifier and feature subset were used to establish the final model. The performance to identify the patients who developed the composite endpoint in the primary and validation cohorts was assessed by the receiver operating characteristic (ROC) curve analysis. Fivefold cross-validation was performed for the machine learning classifier. The model establishment and performance evaluation of machine learning models was performed using the Python 3.7 software. Decision curve analysis was conducted to determine the clinical usefulness by quantifying the net benefits. Other statistical analyses are provided in the Supplementary Material.

Results

Patient characteristics

The main clinical characteristics of patients in the primary and validation cohorts are given in Table 1. The primary cohort that was used to train the DL-based segmentation network and construct the machine learning model consisted of 424 patients recruited from 5 hospitals, and the validation cohort that was used to externally validate the performance of the machine learning model in predicting the development of severe or critical illnesses included 98 patients recruited from 2 hospitals. There was no significant difference between the two cohorts in the prevalence of composite endpoint (8.7% vs.

8.2%, $p = 0.858$). The median duration from symptom onset to CT scan in all patients was 5 (range, 0–23) days.

Lung lesion segmentation and quantification

The original CT images, lung manual and DL-based segmentation, and lesion manual and DL-based segmentation of 3 example cases are illustrated in Fig. 2a, which suggested that the DL-based segmentation framework produced comparable identification of lung and lesion to manual segmentation. ROC curve analysis showed that the DL-based segmentation achieved high accuracy in identifying lesions at the pixel-level, with an AUC of 0.992, which exceeded one of three radiologists and was almost equivalent to another radiologist (Fig. 2b, c). The Dice similarity coefficient of DL-based lesion segmentation was 84.27%, while the Dice similarity coefficients of the three radiologists were 88.51%, 83.73%, and 80.92%, respectively. Furthermore, the lesion region was further subdivided into two different types (GGO and CON) using an unsupervised texture feature clustering approach based on the differences of attenuation and texture (Fig. 2d). The three lesion indicators, namely lesion%, GGO%, and CON%, of each patient in the primary and validation cohorts were yielded (Supplementary Figure 3).

Machine learning classifier and feature selection

Clinical characteristics and CT quantitative measurements among patients according to whether to develop composite endpoint in the primary cohort are shown in Table 2. The correlation matrix heatmap of all 43 features is shown in Fig. 3a. The lesion% and GGO% were significantly and positively correlated with age, alanine aminotransferase (ALT),

Table 1 Clinical characteristics of patients in the primary and validation cohorts

Variables	Primary ($n = 424$)	Validation ($n = 98$)	p value
Age (years)	46 (36–58)	46 (31–53)	0.201
Male gender	210 (49.5%)	51 (52.0%)	0.654
Comorbidities			
Any	107 (25.2%)	21 (21.4%)	0.430
Hypertension	59 (13.9%)	13 (13.3%)	0.866
Diabetes	35 (8.3%)	9 (9.2%)	0.765
Cardiovascular or cerebrovascular disease	19 (4.5%)	6 (6.1%)	0.493
COPD	13 (3.1%)	3 (3.1%)	0.998
Clinical outcomes			
Severe or critical illnesses	37 (8.7%)	8 (8.2%)	0.858
Requiring mechanical ventilation	8 (1.9%)	3 (3.1%)	0.466
ICU admission	14 (3.3%)	4 (4.1%)	0.703
Death	1 (0.2%)	1 (1.0%)	0.341

COPD, chronic obstructive pulmonary disease; *ICU*, intensive care unit; *IQR*, interquartile range

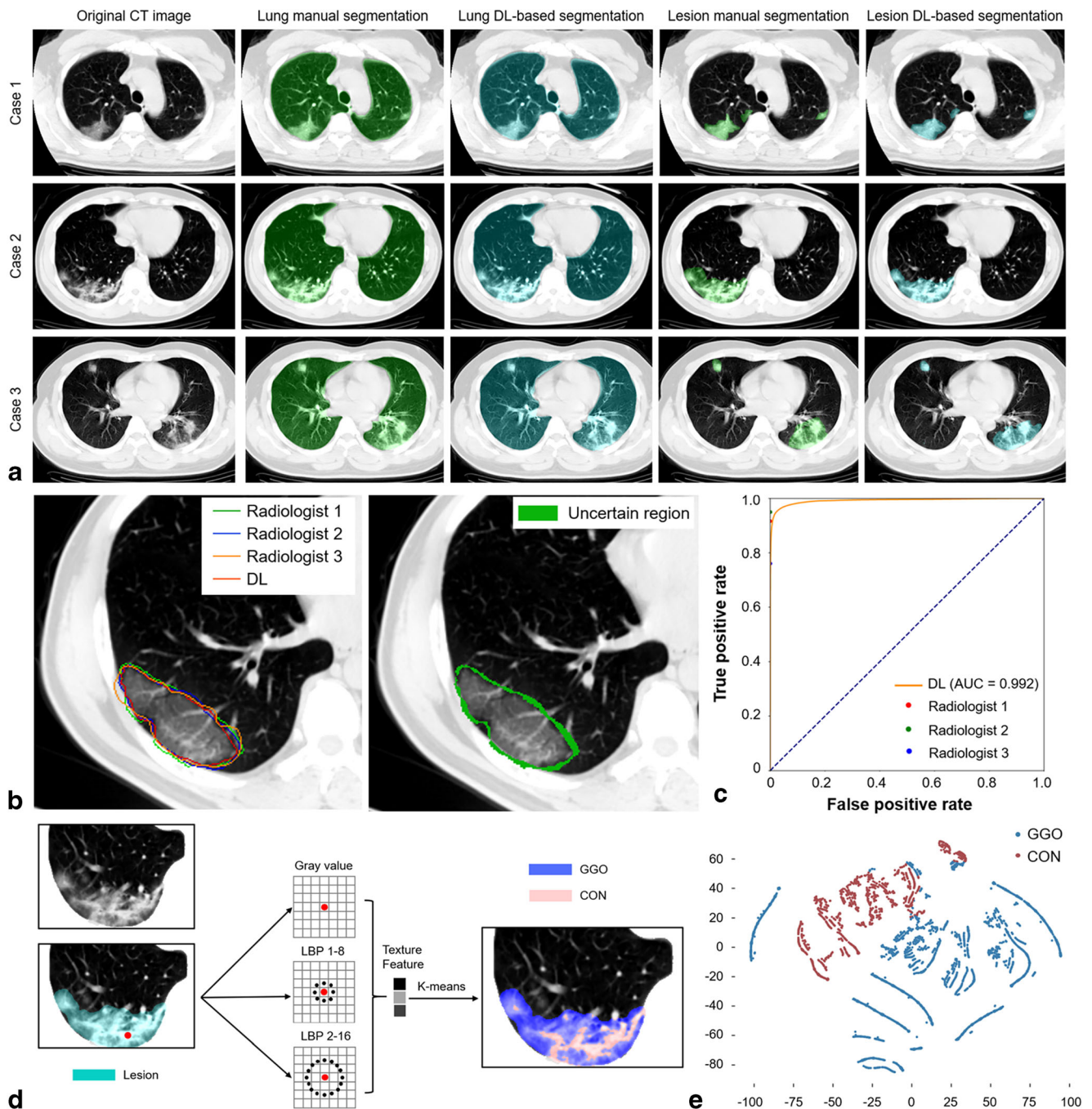Data are presented as median (IQR) or *n* (percentage)

Fig. 2 DL-based lung and lesion segmentation and CT quantitative measurements. **a** The original CT images, lung segmentation, and lesion segmentation of 3 example cases. **b** The contours of 3 radiologists and lesion DL-based segmentation (left) and the uncertain region (right). **c** ROC curve of the pixel-level performance of DL-based segmentation to identify the lesion. **d** Unsupervised multi-scale texture feature clustering to distinguish between GGO and CON based on grey-level attenuation and LBP features. **e** t-SNE plot showing the pixel-level GGO or CON distribution. CON, consolidation; CT, computed tomography; DL, deep learning; GGO, ground-glass opacification; LBP, local binary pattern; ROC, receiver operating characteristic; t-SNE, t-distributed stochastic neighbour embedding

aspartate aminotransferase (AST), blood urea nitrogen (BUN), creatine kinase, lactic dehydrogenase (LDH), and C-reactive protein (CRP) and negatively correlated with lymphocyte count (all $p < 0.01$), while CON% was significantly and positively correlated with AST and LDH (both $p < 0.01$). Considering the unobvious multicollinearity between features

and specific clinical significance of each feature, we included all the features as a candidate feature set.

We compared the performance of five machine learning classifiers based on the candidate feature set in identifying the patients who developed adverse outcomes in the primary cohort and then tested in the validation cohort. Figure 3b depicts the

Table 2 Clinical characteristics and CT quantitative measurements among patients according to whether to develop composite endpoint in the primary cohort

Variables	Yes (n = 37)	No (n = 387)	p value
Age (years)	58 (51–67)	45 (35–56)	< 0.001
Male gender	20 (54.1%)	190 (49.1%)	0.564
Smoking history	7 (18.9%)	33 (8.5%)	0.068
Comorbidities			
Any	25 (67.6%)	82 (21.2%)	< 0.001
Hypertension	11 (29.7%)	48 (12.4%)	0.004
Diabetes	8 (21.6%)	27 (7.0%)	0.006
Cardiovascular or cerebrovascular diseases	7 (18.9%)	12 (3.1%)	0.001
COPD	7 (18.9%)	6 (1.6%)	< 0.001
Symptoms and signs			
Fever	28 (75.7%)	220 (56.8%)	0.026
Cough	24 (64.9%)	199 (51.4%)	0.118
Fatigue or myalgia	8 (21.6%)	84 (21.7%)	0.991
Dyspnea	4 (10.8%)	17 (4.4%)	0.100
Temperature (°C)	37.3 (36.8–38.0)	36.9 (36.5–37.3)	0.001
Heart rate (/min)	90 (80–105)	86 (78–96)	0.092
Respiratory rate (/min)	21 (20–22)	20 (19–20)	0.053
Laboratory findings			
Hemoglobin (g/L)	126.5 (119.3–136.0)	131.0 (120.0–143.0)	0.300
Platelet count ($\times 10^9$/L)	148.0 (119.5–208.0)	174.0 (139.0–228.0)	0.067
White blood cell count ($\times 10^9$/L)	4.5 (3.6–6.0)	4.6 (3.6–5.7)	0.812
Neutrophil count ($\times 10^9$/L)	3.0 (2.4–4.5)	2.9 (2.1–3.7)	0.090
Lymphocyte count ($\times 10^9$/L)	0.9 (0.7–1.3)	1.2 (0.9–1.6)	< 0.001
Monocyte count ($\times 10^9$/L)	0.4 (0.2–0.5)	0.4 (0.3–0.5)	0.618
Total bilirubin (μmol/L)	10.5 (7.1–14.6)	11.9 (8.8–17.3)	0.031
ALT (U/L)	23.0 (16.6–31.2)	19.7 (14.5–28.4)	0.124
AST (U/L)	33.2 (25.8–44.6)	23.0 (18.3–28.3)	< 0.001
Albumin (g/L)	36.8 (34.2–39.8)	39.3 (36.5–42.6)	0.001
BUN (mg/dL)	4.7 (3.8–5.8)	3.9 (3.1–4.8)	0.002
Creatinine (μmol/L)	66.1 (53.8–86.0)	56.4 (44.8–70.0)	0.002
Glucose (mmol/L)	7.2 (5.8–9.2)	5.7 (3.6–4.3)	< 0.001
K^+ (mmol/L)	3.7 (3.5–4.0)	4.0 (3.6–4.3)	0.051
Na^+ (mmol/L)	135.3 (133.0–137.6)	137.5 (135.5–139.9)	< 0.001
INR	1.22 (0.99–1.33)	1.10 (0.90–1.19)	0.043
D-dimer ≥ 0.5 mg/L	16 (43.2%)	47 (12.1%)	< 0.001
Procalcitonin ≥ 0.05 ng/mL	21 (56.8%)	124 (32.0%)	0.002
Hs-cTnI ≥ 28 pg/mL	5 (13.5%)	11 (2.8%)	0.008
Creatine kinase (U/L)	94.0 (40.0–213.5)	72.0 (49.1–109.0)	0.139
LDH (U/L)	265.0 (184.6–342.8)	174.0 (141.3–214.1)	< 0.001
CRP (mg/L)	40.9 (22.9–61.0)	10.4 (2.4–24.5)	< 0.001
PaO$_2$ (mmHg)	71.1 (54.6–106.7)	90.9 (76.0–115.8)	0.009
Radiological findings			
Number of segments involved	16 (12–18)	9 (5–13)	< 0.001
CT severity score	12 (7–17)	6 (3–9)	< 0.001
CT quantitative measurements			
Lesion%	9.5 (3.5–26.6)	3.1 (0.6–7.5)	< 0.001
GGO%	8.2 (3.3–18.9)	2.8 (0.6–6.7)	< 0.001
CON%	1.3 (0.2–2.9)	0.3 (0.0–0.7)	< 0.001

ALT, alanine aminotransferase; *AST*, aspartate aminotransferase; *BUN*, blood urea nitrogen; *CON*, consolidation; *COPD*, chronic obstructive pulmonary disease; *CRP*, C-reactive protein; *CT*, computed tomography; *GGO*, ground-glass opacification; *Hs-cTnI*, hypersensitive cardiac troponin I; *INR*, international normalized ratio; K^+, potassium; LDH, lactic dehydrogenase; Na^+, sodium; *PaO$_2$*, partial pressure of oxygen

ROC curves of all the classifiers and the mean AUC of fivefold cross-validation, sensitivity, specificity, and accuracy are given in Table 3. The XGBoost achieved the highest performance (AUC = 0.964) in the primary cohort, followed by RF (AUC = 0.924), LR (AUC = 0.916), SVM-RBF (AUC = 0.821), and SVM-Linear (AUC = 0.803). Then, the XGBoost classifier was selected as the optimal machine learning classifier. Furthermore, the XGBoost classifier achieved comparable performance (AUC = 0.974) in the validation cohort.

The feature importance rank of each feature in the XGBoost classifier is presented in Fig. 3c and Supplementary Table 2. Then, feature selection was performed in the candidate feature set, as depicted in Fig. 3d. The optimal feature subset containing the top four features, i.e. LDH, presence of comorbidity, lesion%, and hypersensitive cardiac troponin I (hs-cTnI), achieved the highest average AUC, with the minimal number of features.
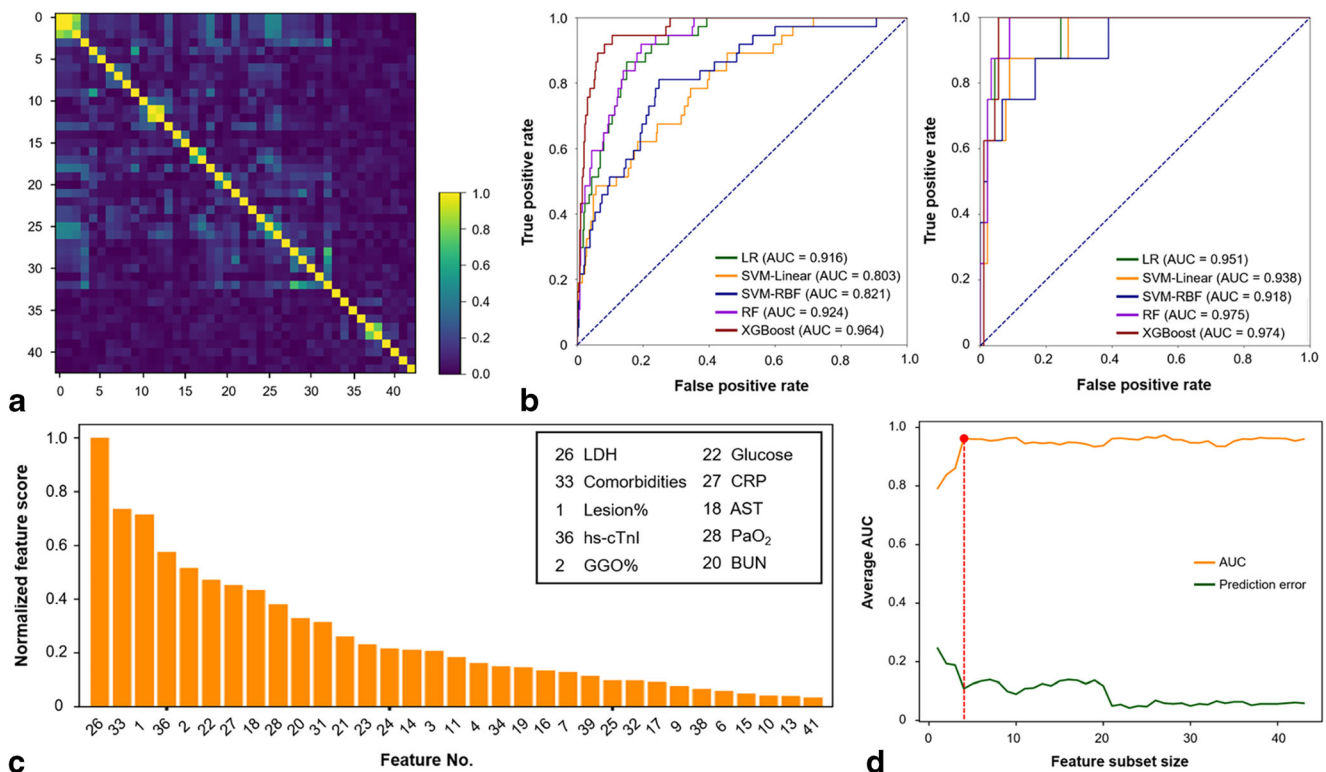
Fig. 3 Optimal machine learning classifier and feature subset selection. **a** The heatmap illustrating the correlations between features in the candidate feature set. **b** The performance of five machine learning classifiers, including LR, SVM-Linear, SVM-RBF, RF, and XGBoost, based on the candidate feature set in the primary cohort (left) and validation cohort (right). **c** The feature importance rank in the XGBoost classifier using fivefold cross-validation in the primary cohort. **d** The relationship between the feature subset size and model performance. The optimal size (red dot) was determined with the highest average AUC and a minimal number of features. The optimal feature subset contained the top 4 features, i.e. LDH, presence of comorbidity, lesion%, and hs-cTnI. AST, aspartate aminotransferase; AUC, area under the receiver operating characteristic curve; BUN, blood urea nitrogen; CRP, C-reactive protein; GGO, ground-glass opacification; hs-cTnI, hypersensitive cardiac troponin I; LDH, lactic dehydrogenase; LR, logistic regression; PaO₂, partial pressure of oxygen; RF, random forest; SVM-Linear, support vector machine with a linear kernel; SVM-RBF, support vector machine with a radial basis function; XGBoost, extreme gradient boosting

Performance evaluation of machine learning model

The XGBoost classifiers based on the optimal feature subset or only three clinical features in the optimal feature subset (i.e. LDH, presence of comorbidity, and hs-cTnI) were then constructed, respectively. The XGBoost classifier based on the top 4 features achieved satisfactory performance in the primary cohort, which was significantly superior to that based on only three clinical features (AUCs = 0.959 and 0.913, respectively; $p = 0.007$). However, no significant difference was found between the two classifiers in the validation cohort (AUCs = 0.953 and 0.881, respectively; $p = 0.216$). The illustration of the ROC curves in the primary and validation cohorts is shown in Fig. 4a, and the detailed model performance is listed in Table 4. The decision curve analysis for the two XGBoost classifiers in the whole cohort is presented in Fig. 4c. Our XGBoost classifier based on the top 4 features had the optimal overall net benefit, the treat-all-patients scheme, and the treat-none scheme across the majority of the range of reasonable threshold probabilities.

Discussion

Our results suggested that DL-based chest CT quantitative measurement could be combined with significant clinical variables to early identify the patients who developed adverse outcomes during hospitalization for patients with COVID-19 using machine learning algorithm. We established an XGBoost classifier incorporating LDH, presence of comorbidity, lesion%, and hs-cTnI which achieved perfectly prediction performance both in the primary and validation cohorts. These findings were derived from DL-based CT quantitative lung injury measurements with sufficient accuracy, stepwise optimal machine learning classifier and feature selection, implemented internal cross-validation and independent external

Table 3 Performance of each classifier based on the candidate feature set in the primary and validation cohorts

Classifier	AUC	Sensitivity	Specificity	Accuracy
Primary cohort				
LR	0.916 (0.885–0.938)	67.6% (25/37)	90.4% (350/387)	0.884 (0.851–0.911)
SVM-Linear	0.803 (0.760–0.838)	51.4% (19/37)	86.0% (333/387)	0.830 (0.790–0.864)
SVM-RBF	0.821 (0.780–0.856)	75.7% (28/37)	84.0% (325/387)	0.833 (0.793–0.866)
RF	0.924 (0.894–0.947)	59.5% (22/37)	93.0% (360/387)	0.901 (0.867–0.927)
XGBoost	0.964 (0.941–0.979)	75.7% (28/37)	96.4% (373/387)	0.946 (0.919–0.965)
Validation cohort				
XGBoost	0.974 (0.910–0.996)	100% (8/8)	85.6% (77/90)	0.867 (0.780–0.925)

AUC, area under the receiver operating characteristic curve; *LR*, logistic regression; *RF*, random forest; *SVM-Linear*, support vector machine with a linear kernel; *SVM-RBF*, support vector machine with a radial basis function; *XGBoost*, extreme gradient boosting

validation, and heterogeneous image data from multiple hospitals; thus, we expect our results to be well generalizable. Hence, when utilized as a supportive decision tool in clinical practice, the proposed prediction of adverse outcomes for COVID-19 could accelerate the early identification of the patients with a high risk of progression enabling faster intervention and likelihood of better outcomes.

Some patients with COVID-19 develop dyspnea and hypoxemia shortly after illness onset and may further progress to ARDS or MODS even death [9]. To early identify the patients who were likely to develop adverse outcomes, our study presented a machine learning model incorporating four clinical or imaging variables, with perfect performance in the primary and validation cohorts, respectively. Zhang et al developed a clinically applicable AI-assisted model to predict the progression to critical illness with AUC, sensitivity, and specificity of 0.909, 86.71%, and 80.00%, respectively, which identified the quantitative lesion features as the most significant contributor in the clinical prognosis estimation as well as some clinical parameters relating to multiple tissues/organs function and systemic homeostasis [14]. Compared with their work, we built a model incorporating fewer significant features for clinical use, slightly improved the prediction performance, and validated these findings in an independent external cohort. As for the difference in the most important features of the machine learning model between our study and theirs, this

may be explained by the differences in the machine learning algorithm adopted and study endpoint.

Previous studies reported some feasible prognostic model for the prediction of developing severe COVID-19, particularly the CALL score [11, 19]. Similar to our results, the CALL score also included four high-risk factors associated with COVID-19 progression, i.e. underlying comorbidity, age, LDH, and lymphocyte count. In our XGBoost classifier, CT-derived lesion% and hs-cTnI were also included apart from LDH and presence of comorbidity. In general, the top four features in our model were associated with multiple tissues/organs dysfunction, lung injury, and declined organ reserve function, respectively. LDH is an intracellular cytoplasmic enzyme that is widely expressed in multiple tissues and has been reported as a predictor of disease severity in several clinical conditions [20, 21]. COVID-19 involves multiple organs or systems, including the gastrointestinal tract, liver, kidney, cardiovascular system, and nervous system [22–24]. Damage to the liver, kidney, or lung in severe attacks may contribute to the cellular death and LDH leakage with consequently raised serum LDH levels in COVID-19. Meanwhile, hs-cTnI is the best laboratory parameter inflecting cardiac involvement with COVID-19, which could prompt early initiation of measures to improve tissue oxygenation. Elevated hs-cTnI concentration may be due to non-ischemic causes of myocardial injury or type 2 myocardial infarction, of which

Table 4 Performance of the XGBoost classifiers in the primary and validation cohorts

Cohort	AUC	Sensitivity	Specificity	Accuracy
Primary cohort				
Top four features	0.959 (0.936–0.976)	89.2% (33/37)	91.5% (354/387)	0.913 (0.882–0.936)
Three clinical features	0.913 (0.882–0.938)	75.7% (28/37)	90.7% (351/387)	0.894 (0.861–0.920)
Validation cohort				
Top four features	0.953 (0.891–0.986)	100% (8/8)	87.8% (79/90)	0.888 (0.810–0.936)
Three clinical features	0.881 (0.800–0.938)	75.0% (6/8)	87.8% (79/90)	0.867 (0.786–0.921)

AUC, area under the receiver operating characteristic curve; *XGBoost*, extreme gradient boosting
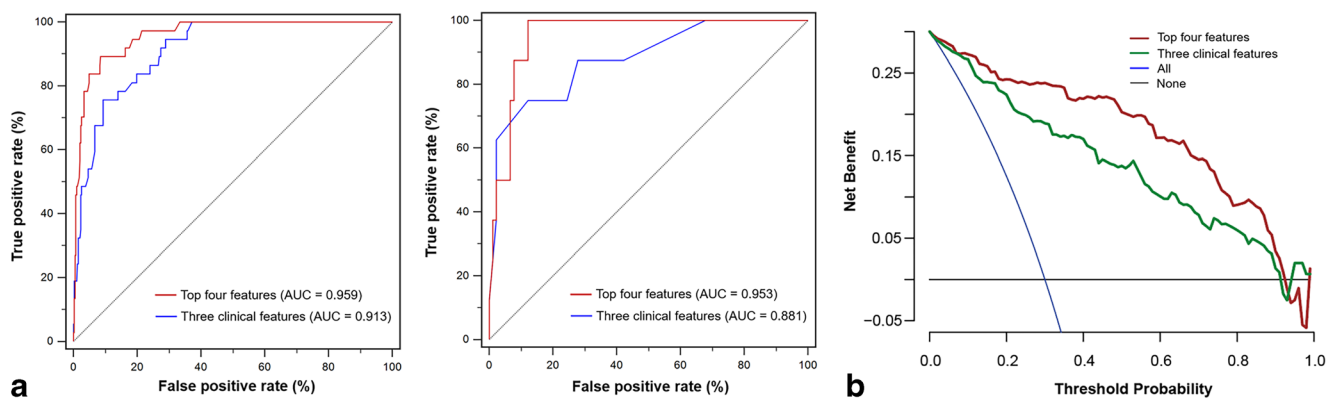
Fig. 4 Performance of the XGBoost classifiers based on the top four features or only three clinical features. **a** ROC curves of the XGBoost classifiers in the primary cohort (left) and validation cohort (right). **b** Comparison of decision curves of the XGBoost classifiers in the whole cohort. AUC, area under the receiver operating characteristic curve; ROC, receiver operating characteristic; XGBoost, extreme gradient boosting

the prevalence is likely to increase in patients affected by COVID-19 [25]. Besides, it is the sensitivity of hs-cTnI testing that ensures it is one of the earliest and most precise indicators of organ dysfunction [26]. The significance of LDH and hs-cTnI as risk factors in predicting the development of ARDS or mortality has also been proposed in previous reports [9, 27]. CT-derived lesion% is a quantitative indicator directly obtained on DL-based lesion segmentation, which is associated with the extent of pulmonary infection by SARS-CoV-2. Lung involvement in COVID-19 reflects the most serious degree of damage caused by the coronavirus on various organs or systems. Furthermore, chronic comorbidity has been shown to be an independent prognostic factor associated with unfavourable outcomes in many reports [27, 28]. As expected, our analysis revealed that underlying comorbidity played an important role in the clinical progression in COVID-19 patients, which may be explained by the overactivation of the renin-angiotensin system (RAS) and enhanced susceptibility to pulmonary edema by the exhaustion of angiotensin-converting enzyme 2 (ACE2), which is the functional receptor for the SARS-CoV-2 spike protein [29, 30]. Recently, Liang et al proposed a clinical risk score incorporating 10 clinical variables to predict the occurrence of critical illness in hospitalized patients with COVID-19 [19]. By contrast, we adopted DL-derived CT quantitative measurements to accurately assess the degree of lung injury and aimed to early predict the adverse outcomes in patients with non-severe COVID-19 pneumonia on admission, and our findings further suggested that CT-derived lesion% played an important role in our XGBoost machine learning model.

To analyze the composition proportions of lung lesions, we innovatively proposed an unsupervised multi-scale texture feature clustering to distinguish GGO and CON without the need of prior annotated data for training for further quantification. Shi et al found that COVID-19 pneumonia manifested with dynamic CT abnormalities during disease evolution, with

focal unilateral to diffuse bilateral GGOs that progressed to or co-exist with CONs [13]. Thus, we speculated that the extent or proportion of GGO and CON may contribute to early predicting the disease evolution. According to our results, GGO% ranked the fifth important features in identifying patients who were likely to develop severe or critical illnesses. However, to simplify the machine learning classifier with sufficient accuracy, we only included the top 4 features in our final model. Another study showed that the average infection attenuation of lung abnormalities computed automatically by a deep learning–based AI system could distinguish between the severe and non-severe COVID-19 stages [31]. However, we did not use the average attenuation of lesion to discriminate between GGO and CON in our study since there is no recognised reference threshold value. Besides, CT severity score, a semi-quantitative index associated with the lung involvement, also has been subjectively estimated and included in the candidate feature set. However, the feature importance rank indicated that the radiologist-derived CT severity score was inferior to these DL-derived CT quantitative measurements, which provides more accurate, objective, and reproducible quantification of lung involvement.

There were some limitations in our study. First, the study was retrospectively conducted and the laboratory tests were clinically driven and not systematic, which resulted in incomplete laboratory tests results in some cases. Second, the cytokine storm is the hallmark of severe ill COVID-19, which is characterized by increased amounts of serum proinflammatory cytokines [32]. The detection of cytokines may have added a further dimension to this study. Third, the utility of our model is limited by unavailable open-source segmentation software and lack of easy-to-use online tool. Also, the selection of the optimal machine learning classifier was subjective. Finally, the proportions of patients who reached the composite endpoint in the primary or validation cohorts were about 8%. Although we employed class weight adjustment to reduce the impact of

imbalanced samples on the prediction performance of the machine learning classifier, our established model may be limited by the potential overfitting risk and specific cohort characteristics. The possibility to extrapolate our model to other patient populations needs to be confirmed by a larger sample.

In summary, our study presented a machine learning model incorporating four clinical or imaging variables at the time of admission with high accuracy to identify the patients who developed adverse outcomes during hospitalization, which could be used to facilitate the prediction of adverse outcomes in patients with COVID-19. Our findings may allow efficient utilization of medical resources and individualized treatment plans for COVID-19 patients.

Declarations

Guarantor The scientific guarantor of this publication is Zhichao Feng, M.D.

Conflict of interest The authors of this manuscript declare no relationships with any companies whose products or services may be related to the subject matter of the article.

Statistics and biometry Hongzhuan Tan kindly provided statistical advice for this manuscript.

Informed consent Written informed consent was waived by the Institutional Review Board.

Ethical approval Institutional Review Board approval from the Ethics Committee of The Third Xiangya Hospital of Central South University (Changsha, China) was obtained.

Methodology
• retrospective
• case-control study/diagnostic or prognostic study
• multicentre study

References

1. Guan WJ, Ni ZY, Hu Y et al (2020) Clinical characteristics of coronavirus disease 2019 in China. N Engl J Med 382:1708–1720
2. Yang X, Yu Y, Xu J et al (2020) Clinical course and outcomes of critically ill patients with SARS-CoV-2 pneumonia in Wuhan, China: a single-centered, retrospective, observational study. Lancet Respir Med 8:475–481
3. Feng Y, Ling Y, Bai T et al (2020) COVID-19 with different severities: a multicenter study of clinical features. Am J Respir Crit Care Med 201:1380–1388
4. Wang Y, Zhang D, Du G et al (2020) Remdesivir in adults with severe COVID-19: a randomised, double-blind, placebo-controlled, multicentre trial. Lancet 395:1569–1578
5. Grein J, Ohmagari N, Shin D et al (2020) Compassionate use of remdesivir for patients with severe Covid-19. N Engl J Med 382: 2327–2336
6. Hung IF, Lung KC, Tso EY et al (2020) Triple combination of interferon beta-1b, lopinavir-ritonavir, and ribavirin in the treatment of patients admitted to hospital with COVID-19: an open-label, randomised, phase 2 trial. Lancet 395:1695–1704
7. Feng Z, Li J, Yao S et al (2020) Clinical factors associated with progression and prolonged viral shedding in COVID-19 patients: a multicenter study. Aging Dis 11:1069–1081
8. Sanders JM, Monogue ML, Jodlowski TZ, Cutrell JB (2020) Pharmacologic treatments for coronavirus disease 2019 (COVID-19): a review. JAMA 323:1824–1836
9. Wu C, Chen X, Cai Y et al (2020) Risk factors associated with acute respiratory distress syndrome and death in patients with coronavirus disease 2019 pneumonia in Wuhan, China. JAMA Intern Med 180: 934–943
10. Wynants L, Van Calster B, Collins GS et al (2020) Prediction models for diagnosis and prognosis of covid-19 infection: systematic review and critical appraisal. BMJ 369:m1328
11. Ji D, Zhang D, Xu J et al (2020) Prediction for progression risk in patients with COVID-19 pneumonia: the CALL score. Clin Infect Dis 71:1393–1399
12. Feng Z, Yu Q, Yao S et al (2020) Early prediction of disease progression in COVID-19 pneumonia patients with chest CT and clinical characteristics. Nat Commun 11:4968
13. Shi H, Han X, Jiang N et al (2020) Radiological findings from 81 patients with COVID-19 pneumonia in Wuhan, China: a descriptive study. Lancet Infect Dis 20:425–434
14. Zhang K, Liu X, Shen J et al (2020) Clinically applicable AI system for accurate diagnosis, quantitative measurements, and prognosis of COVID-19 pneumonia using computed tomography. Cell 181: 1423–1433 e1411
15. Collins GS, Reitsma JB, Altman DG, Moons KG (2015) Transparent Reporting of a multivariable prediction model for Individual Prognosis or Diagnosis (TRIPOD): the TRIPOD statement. Ann Intern Med 162:55–63
16. Gao K, Su J, Jiang Z et al (2021) Dual-branch combination network (DCN): towards accurate diagnosis and lesion segmentation of COVID-19 using CT images. Med Image Anal 67:101836
17. Xie C, Yang P, Zhang X et al (2019) Sub-region based radiomics analysis for survival prediction in oesophageal tumours treated by definitive concurrent chemoradiotherapy. EBioMedicine 44:289–297
18. Angraal S, Mortazavi BJ, Gupta A et al (2020) Machine learning prediction of mortality and hospitalization in heart failure with preserved ejection fraction. JACC Heart Fail 8:12–21
19. Liang W, Liang H, Ou L et al (2020) Development and validation of a clinical risk score to predict the occurrence of critical illness in hospitalized patients with COVID-19. JAMA Intern Med 180: 1081–1089
20. Yang Z, Dong L, Zhang Y et al (2015) Prediction of severe acute pancreatitis using a decision tree model based on the revised atlanta classification of acute pancreatitis. PLoS One 10:e0143486
21. Muchtar E, Dispenzieri A, Lacy MQ et al (2017) Elevation of serum lactate dehydrogenase in AL amyloidosis reflects tissue damage and is an adverse prognostic marker in patients not eligible for stem cell transplantation. Br J Haematol 178:888–895

22. Cheung KS, Hung IFN, Chan PPY et al (2020) Gastrointestinal manifestations of SARS-CoV-2 infection and virus load in fecal samples from a Hong Kong cohort: systematic review and meta-analysis. Gastroenterology 159:81–95

23. Lei F, Liu YM, Zhou F et al (2020) Longitudinal association between markers of liver injury and mortality in COVID-19 in China. Hepatology 72:389–398

24. Zheng YY, Ma YT, Zhang JY, Xie X (2020) COVID-19 and the cardiovascular system. Nat Rev Cardiol 17:259–260

25. Hammadah M, Kim JH, Tahhan AS et al (2018) Use of high-sensitivity cardiac troponin for the exclusion of inducible myocardial ischemia: a cohort study. Ann Intern Med 169:751–760

26. Chapman AR, Bularga A, Mills NL (2020) High-sensitivity cardiac troponin can be an ally in the fight against COVID-19. Circulation 141:1733–1735

27. Du RH, Liang LR, Yang CQ et al (2020) Predictors of mortality for patients with COVID-19 pneumonia caused by SARS-CoV-2: a prospective cohort study. Eur Respir J 55:2000524

28. Chen R, Liang W, Jiang M et al (2020) Risk factors of fatal outcome in hospitalized subjects with coronavirus disease 2019 from a nationwide analysis in China. Chest 158:97–105

29. Vaduganathan M, Vardeny O, Michel T, McMurray JJV, Pfeffer MA, Solomon SD (2020) Renin-angiotensin-aldosterone system inhibitors in patients with Covid-19. N Engl J Med 382:1653–1659

30. Touyz RM, Li H, Delles C (2020) ACE2 the Janus-faced protein - from cardiovascular protection to severe acute respiratory syndrome-coronavirus and COVID-19. Clin Sci (Lond) 134:747–750

31. Li Z, Zhong Z, Li Y et al (2020) From community-acquired pneumonia to COVID-19: a deep learning-based method for quantitative analysis of COVID-19 on thick-section CT scans. Eur Radiol 30:6828–6837

32. Huang C, Wang Y, Li X et al (2020) Clinical features of patients infected with 2019 novel coronavirus in Wuhan, China. Lancet 395:497–506